Nutrition Research and Practice 2019;13(2):95-104

http://e-nrp.org

Anti-inflammatory effect of Lycium barbarum on polarized human intestinal epithelial cells

So-Rok Lee[1], Hye-Jeong Hwang[2], Ju-Gyeong Yoon[1], Eun-Young Bae[3], Kyo-Suk Goo[4], Sang-Joon Cho[4] and Jin Ah Cho[1§]

[1]Department of Food and Nutrition, Chungnam National University, 99, Daehak-ro, Yuseong-gu, Daejeon 34134, Korea
[2]Department of Agrofood Resources, National Institute of Agricultural Sciences, RDA, Wanju, Jeonbuk 55365, Korea
[3]Elohim Co. R&D Center, Daejeon 34025, Korea
[4]Application Technology Center, Park System, Suwon, Gyeonggi 16229, Korea

BACKGROUND/OBJECTIVES: Inflammatory Bowel Disease (IBD) has rapidly escalated in Asia (including Korea) due to increasing westernized diet patterns subsequent to industrialization. Factors associated with endoplasmic reticulum (ER) stress are demonstrated to be one of the major causes of IBD. This study was conducted to investigate the effect of *Lycium barbarum* (*L. barbarum*) on ER stress.
MATERIALS/METHODS: Mouse embryonic fibroblast (MEF) cell line and polarized Caco-2 human intestinal epithelial cells were treated with crude extract of the *L. chinense* fruit (LF). Paracellular permeability was measured to examine the effect of tight junction (TJ) integrity. The regulatory pathways of ER stress were evaluated in MEF knockout (KO) cell lines by qPCR for interleukin (IL) 6, IL8 and XBP1 spliced form (XBP1s). Immunoglobulin binding protein (BiP), XBP1s and CCAAT/enhancer-binding homologous protein (CHOP) expressions were measured by RT-PCR. Scanning Ion Conductance Microscopy (SICM) at high resolution was applied to observe morphological changes after treatments.
RESULTS: Exposure to LF extract strengthened the TJ, both in the presence and absence of inflammation. In polarized Caco-2 pretreated with LF, induction in the expression of proinflammatory marker IL8 was not significant, whereas ER stress marker XBP1s expression was significantly increased. In wild type (wt) MEF cells, IL6, CHOP and XBP1 spliced form were dose-dependently induced when exposed to 12.5-50 μg/mL extract. However, absence of XBP1 or IRE1α in MEF cells abolished this effect.
CONCLUSION: Results of this study show that LF treatment enhances the barrier function and reduces inflammation and ER stress in an IRE1α-XBP1-dependent manner. These results suggest the preventive effect of LF on healthy intestine, and the possibility of reducing the degree of inflammatory symptoms in IBD patients.

Nutrition Research and Practice 2019;13(2):95-104; https://doi.org/10.4162/nrp.2019.13.2.95; pISSN 1976-1457 eISSN 2005-6168

Keywords: Lycium barbarum, ER stress, inflammation

INTRODUCTION

Endoplasmic reticulum (ER) plays a major role in protein synthesis, folding and processing of secretory and transmembrane proteins [1,2]. ER stress is caused by the accumulation of misfolded or unfolded proteins in ER due to genetic or environmental factors [3]. This process is mediated by three ER transmembrane domains: IRE1, PERK and ATF6, which induce the Unfolded Protein Response (UPR). First, translational attenuation due to PERK-dependent phosphorylation of eIF2 occurs to overcome the burden of ER [4]. Failure of this process induces UPR-related genes, primarily chaperones such as the immunoglobulin binding protein (BiP, a 78 kDa glucose control protein GRP78) and 74 kDa glucose control protein (GRP74), to prevent further accumulation of unfolded and/or misfolded proteins, with simultaneous transcriptional activation of the UPR genes such as IRE1α / XBP1 and AFT6. Activation of IRE1α by ER stress results in generation of the XBP1 spliced form by inducing the endonuclease domain of IRE1α to cleave the 26-nt intron from full-length XBP1 mRNA [5]. Persistence of the problem results in abnormal proteins in the ER being extracted, reversed to the cytoplasm, and degraded by an ER related Associated Degradation (ERAD) system consisting of ubiquitin-dependent proteasomes [6]. This stimulates the nuclear factor kappa light chain-enhancer of activated B cells (NF-κB), a transcription factor mediating immunity and anti-apoptotic responses. Irreversible cellular damage and insufficient pro-survival activity of the UPR for the retention of cellular homeostasis results in induction of apoptosis by stimulation of the CCAAT/enhancer-binding homologous protein (CHOP) and activation of the JNK (c-Jun

This research was supported by the Ministry of Education of the Republic of Korea and the National Research Foundation of Korea (NRF-2016-1964-01) and Chungnam National University Research grant. We thank to the Zebrafish Center for Disease Modeling (ZCDM), Daejeon, Korea for providing the wild type zebra fish and eggs as well as valuable advice and guidance.
§ Corresponding Author: Jin Ah Cho, Tel. 82-42-821-6833, Fax. 82-42-821-8887, Email. jacho@cnu.ac.kr
Received: October 30, 2018, Revised: November 16, 2018, Accepted: December 26, 2018

N-terminal kinase) kinase and caspase-12 [7,8].

ER stress and UPR are critical to intestinal cells, and damage to UPR signaling leads to chronic inflammatory diseases such as Inflammatory Bowel Disease (IBD), Rheumatoid Bowel Syndrome (IBS), and Necrotizing Enterocolitis (NEC) [9,10].

Asian countries have seen a dramatic increase in IBD incidence due to westernized diet patterns [11]. IBD is a complex disease caused by several genetic and environmental factors. The cause of Crohn's Disease (CD) and Ulcerative Colitis (UC), two principal types of IBD, are intestinal inflammation and ER stress, especially in the ileum and/or colonic epithelia [12,13]. Inflammatory symptoms are augmented by diet patterns such as gluten sensitivity, alterations in the gut microbiome, breach of intestinal barrier and genetic susceptibility [14]. Breach of intestinal barrier and alteration of the gut microbiome cause dysfunction of the innate immune system such as toll-like receptors [15]. Genome-Wide Association Study has confirmed 163 IBD susceptibility loci related to 300 known genes, which in turn are associated with cytokine induction, lymphocyte activation, response to bacterial infection, and ER stress [16-19]. Hence, IBD patients have increased levels of cytokines such as tumor necrosis factor-alpha (TNFα), interferon-gamma (IFNɣ), interleukin (IL) 1β, IL6 and IL17 [20]. Furthermore, due to loss of integrity of the intestinal epithelium, nutritional deficiencies (such as malabsorption, diarrhea, and intestinal blood loss) are common features of IBD patients. Therefore, dietary interventions are extremely important for these patients, which include certain vitamins and mineral replacement therapy, low fiber diets and low-FODMAP diet (the global restriction of all fermentable carbohydrates) [21-23]. Recent alternative approaches use alternative medicines for IBD therapy [24]. Herbal therapy with curcumin in UC, and wormwood in CD, were explored for IBD patients [25,26].

Although a native plant grown only in the Ningxia Hui Autonomous Region of north-central China, *Lycium barbarum* (*L. barbarum*) has gained considerable attention as a superfood in the western countries [27]. It has long been used as an edible and traditional medicinal plant in eastern countries such as China and Korea [28]. Fresh or dried fruits are used as food, and leaves are used as food or tea. Of the various components of LF, the *L. barbarum* polysaccharides (LBP) are the most well-studied. Other components include carotenoids and their related compounds, betaine, cerebroside, β-sitosterol, p-coumaric acid, and vitamins [29]. *L. barbarum* has been administered for the treatment of diabetes and hyperlipidemia, for reducing blood sugar and serum lipids, respectively, and is also known to exert its effects of neuroprotection and antioxidants [30-33]. However, the outcomes of LF on ER stress and oxidative stress on intestinal epithelial cells are not well known. This study was therefore undertaken to investigate the anti-inflammatory effects of LF associated to the ER stress pathway on polarized human intestinal epithelial cells.

MATERIALS AND METHODS

Materials

Dried 5 kg of LF was harvested from the Ningxia Hui Autonomous Region of north-central China; extraction was performed for 7 days by adding 70% alcohol to make 8 times of the weight. The resultant extract was filtered, concentrated in a rotary evaporator, and used in this study.

Cell culture and cell viability

Human intestinal epithelial Caco-2 cells and mouse embryonic fibroblast (MEF) cell lines (American Type Culture Collection, USA) were cultured in Dulbecco's modified Eagle's medium (DMEM, Gibco, USA) supplemented with 10% heat-inactivated fetal bovine serum (FBS, Gibco, Grand Island, NY, USA) and 1% Penicillin-Streptomycin solution (P/S, Sigma-Aldrich Co., USA) at 37℃ under humidified 5% CO_2. Caco-2 polarization was performed as follows: 24-well Transwell (35024, SPL, Korea) dishes were coated with 396 μg/cm^2 collagen, seeded with Caco-2 cells, and monolayers were grown for 10 days. The experiment was performed when the Transepithelial/Transendothelial Electrical Resistance (TEER) reached a value in the range of 500-600 Ωcm^2. LF stock solution (100 mg/mL) was made by dissolving 100 mg of the dry crude extract in 1 mL DMSO. Cell viability was determined by the WST assay kit (EZ-cytox, Daeil lap service Co. Ltd., Seoul, Korea). Caco-2 cells were seeded in 96-well plate and incubated for 24 hours (h) under the same culture conditions previously mentioned. Cells were pretreated with various concentrations of LF (0, 12.5, 25, 50, 100 and 250 μg/mL) for 24 h followed by WST assay, according to the manufacturer's instruction. Absorbance was measured at 450 nm on a micro-plate reader (xMark™ Microplate Absorbance Spectrophotometer, Bio-Rad Inc., Hercules, California, USA) after 3 h.

RNA extraction and cDNA synthesis

Total RNA was extracted from polarized Caco-2 cells and MEF cell lines. Briefly, after removal of the cell medium, Tri-reagent (MRC Inc., Cincinnati, USA) was added to each well and the resultant lysates were harvested. Chloroform was then added, and the mixture was centrifuged at 12,000 g for 15 minutes at 4℃. The supernatant was separated, mixed with isopropanol, and centrifuged at 12,000 g at 20℃ for 8 minutes. RNA pellets were harvested, and the RNA concentration was measured

Table 1. Real-Time qPCR primer sequences

Gene	Primer	Sequence (5′→ 3′)
Human		
GAPDH	Forward	ATG GGG AAG GTG AAG GTC G
	Reverse	GGG GTC ATT GAT GGC AAC AAT A
XBP1s	Forward	AAC CAG GAG TTA AGA CAG CGC TT
	Reverse	CTG CAC CCT CTG CGG ACT
IL8	Forward	GGG GTC ATT GAT GGC AAC AAT A
	Reverse	CAT GAA GTG TTG AAG TAG ATT TGC TTG
Mouse		
ß-actin	Forward	GGC TGT ATT CCC CTC CAT CG
	Reverse	CCA GTT GGT AAC AAT GCC ATG T
XBP1s	Forward	GAG TCC GCA GCA GGT G
	Reverse	GTG TCA GAG TCC ATG GGA
IL-6	Forward	CTG CAA GAG ACT TCC ATC CAG
	Reverse	AGT GGT ATA GAC AGG TCT GTT GG

GAPDH, glyceraldehyde-3-phosphate dehydrogenase; XBP1s, X-box binding protein 1 spliced form; IL, interleukin.

Table 2. RT-PCR primer sequence

Gene	Primer	Sequence (5′→ 3′)
Mouse		
ß-actin	Forward	GGG TCA GAA GGA TTC CTA TG
	Reverse	GGT CTC AAA CAT GAT CTG GG
XBP1s	Forward	ACA CGC TTG GGA ATG GA CAC
	Reverse	CCA TGG GAA GAT GTT CTG GG
CHOP	Forward	CAC ATC CCA AAG CCC TCG CTC TC
	Reverse	TCA TGC TTG GTG CAG GCT GAC CAT
BiP	Forward	CTG GGT ACA TTT GAT CTG ACT GG
	Reverse	GCA TCC TGG TGG CTT TCC AGC CAT TC

XBP1s, X-box binding protein 1 spliced form; CHOP, CCAAT/enhancer-binding homologous protein; BiP, Immunoglobulin binding protein.

using Nano Drop (Nano Drop ONE, Thermo Scientific Inc., USA), after which cDNA was synthesized using the RT-Kit (M-MLV, RNase H -, BioFACT Co., Korea).

Real-time qPCR

The synthesized cDNA was analyzed by the real-time PCR system using 2X Real-Time PCR Master Mix kit (Including SYBR Green, Low ROX, BioFACT Co., Korea) according to manufacturer's instruction. Amplification was performed for 45 cycles. Data analysis was performed using the Agilent AriaMX 1.0 program. The primer sequences used in the experiments are presented in the Table 1.

Reverse transcription-PCR

In order to measure mRNA expression of the X-box binding protein 1 spliced form (XBP1s), reverse transcription (RT)-PCR was performed according to the manufacturer's instruction (2X Taq Basic PCR Master Mix2, BioFACT Co., Korea). The primer sequences used in the experiments are presented in Table 2. The samples were loaded onto a 3% agarose gel for electrophoresis and verified under UV light (AE-9000 E-Graph, ATTO, Japan).

Paracellular permeability

Caco-2 cells polarized for 10 days were pretreated with LF extract for 24 h, followed by exposure to a cytokine cocktail (50 ng/mL TNF-α + 50 ng/mL IFN-γ + 25 ng/mL IL-1β + 10 μg/mL LPS) applied on the apical side of the chamber for an additional 24 h. Apical and basal side were then washed with HBSS (Hanks' balanced salts, Sigma-Aldrich Co., USA) supplemented with 10 mM HEPES (Sigma-Aldrich Co., USA). Fresh HBSS/HEPES was added to the basal side, and 4 kDa fluorescein isothiocyanate dextran (FITC-dextran, Sigma-Aldrich Co., Sweden) diluted with HBSS/HEPES solution to a final concentration of 1 mg/mL was added to the apical chamber and incubated for 72 h. At the indicated time point, the basal solutions were collected and the fluorescence signal was detected using a DTX 800 multimode detector (DTX800, Beckman Coulter Inc., Brea, CA, USA) at excitation wavelength of 490 nm and emission wavelength of 520 nm.

LF treatment on Zebrafish embryo

Wild type (wt) zebrafish (*D. rerio*) were maintained at the Chungnam National University (CNU-01027) as per the Animal Research Guidelines. Wild type zebra fish and/or eggs were provided by the Zebrafish Center for Disease Modeling (ZCDM), Korea. At 2 to 75 h post-fertilization (hpf), zebrafish embryos were isolated in 24-well plates (10 embryos/well) in 1 mL standard egg water (0.1%) supplemented with methylene blue, then they were exposed to LF (0, 12.5, 25, 50, 100, 250 μg/mL) for various times as indicated. The LF solutions were changed once every 24 h. Embryos were imaged until hatching, using the Leica microscope (DM2000, Leica co., Wetzlar, Germany) and Canon microscope (SZ2-ILST, Tokyo, Japan).

Scanning ion-conductance microscopy (SICM)

SICM images were obtained with a commercial SPM (NX- 12 system, Park Systems Corp, Suwon, Korea). This system has a Scanning Probe Microscope system fixed on top of an inverted optical microscope (Eclipse Ti, Nikon Corp., Tokyo, Japan) enabling to view the bottom side of the sample and acquire SICM images simultaneously. The SPM system has a 100 μm × 100 μm xy flat scanner, and a separate SICM head with a 15 μm z scanner. The SICM probe consists of a glass pipette filled with electrolyte, and an Ag/AgCl pipette electrode inserted into it. The SICM probe is fabricated from borosilicate capillaries (inner diameter 0.58 mm, outer diameter 1.0 mm, Warner Instruments, Hamden, CT, USA) using a CO_2-laser-based micropipette puller (P-2000, Sutter Instruments, Novato, CA, USA); the inner and outer diameters of the tip of the SICM probe are approximately 80 nm and 160 nm, respectively. In the present study, the surface profiles of fixed single cell images were primarily obtained using the Approach-Retract Scanning (ARS) mode of the SICM to ensure non-destructive high resolution surface images.

Statistical analysis

Data from all experiments were analyzed using the SPSS/Windows 24.0 (SPSS Inc., Chicago, USA) program. All experiments were carried out more than 3 times. Results are expressed as mean ± SD. Student's t-test was used to obtain the mean difference between two groups, and One-way ANOVA was used for two or more groups. After ANOVA analysis, Duncan's multiple range test was applied to identify differences between groups. A P-value < 0.05 is considered statistically significant.

RESULT

In vitro and in vivo toxicity of LF extract

To investigate the effect of LF on cell viability, WST assay was performed on Caco-2 cells (a human colon epithelial cell line). This assay converts the dehydrogenated and water-soluble tetrazolium of living cells to a detectable aqueous soluble formazan (orange color), thereby identifying cell proliferation. No change in cell viability was observed after exposing the cells to LF extract for 24 h, suggesting that the extract is non-toxic in the range 0-250 μg/mL LF *in vitro* (Fig. 1A).

To examine the *in vivo* toxicity of LF, zebra fish embryos treated with different concentrations of LF dissolved in egg water were observed for development and documented at each time point (Fig. 1B). No deterioration of embryo development

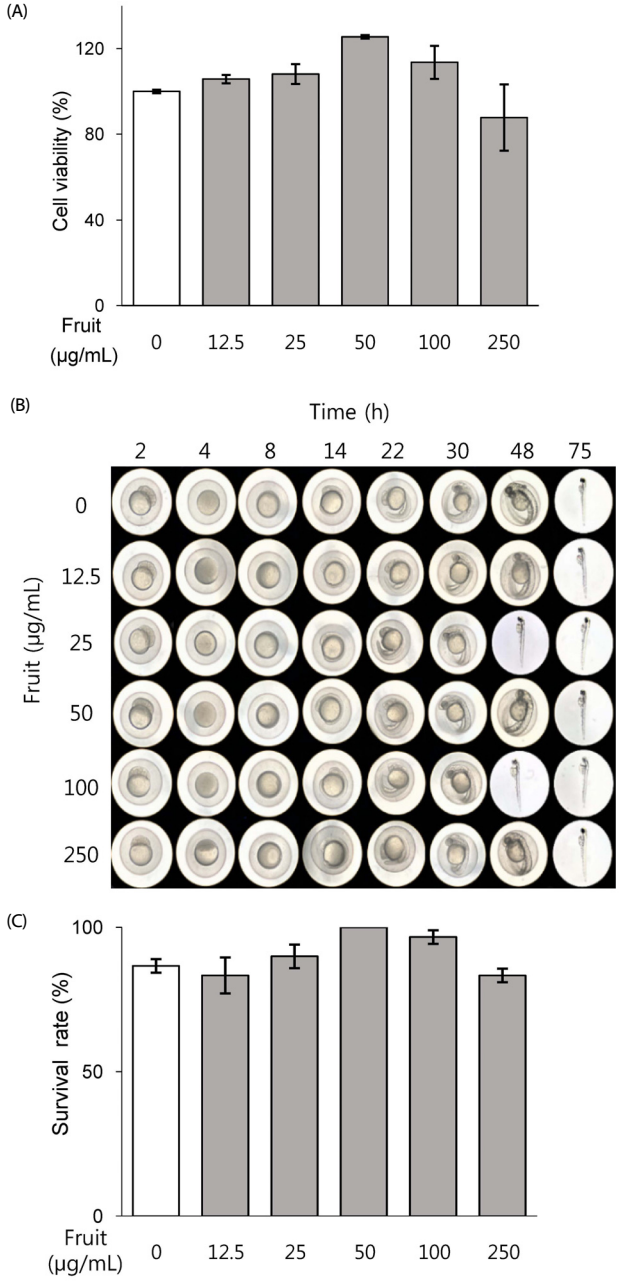

Fig. 1. Effect of LF on cell viability *in vitro* and *in vivo*. Human intestinal epithelial cells (Caco-2) were pretreated with different concentrations of LF (0, 12.5, 25, 50, 100, 250 μg/mL) for 24 h (A) to evaluate for cell viability. Zebra fish eggs were pretreated with same concentrations for 75 h to evaluate toxicity (B) and survival rate (C). The experiments were performed individually at least three times. Data are expressed as mean ± SD. In Fig. 1A, the inter-concentration statistics were analyzed by One-way ANOVA. White bar represents the negative control.

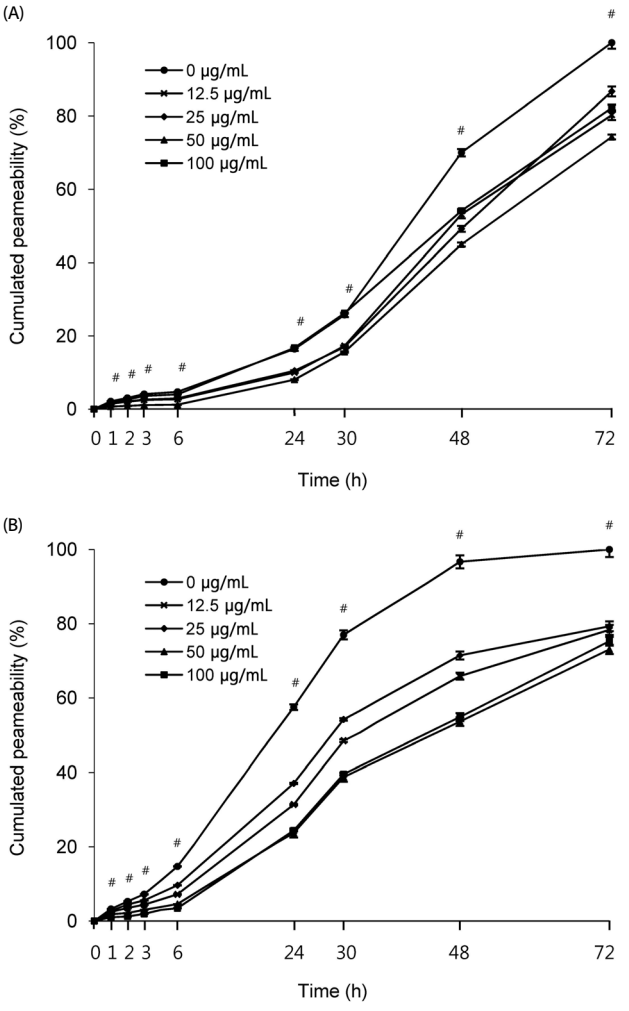

Fig. 2. Protective effect of LF on cell permeability of Caco-2 cells. Polarized Caco-2 cells were pretreated with indicated concentrations of LF for 24 h, followed by the absence (A) or presence (B) of cytokine cocktail (50 ng/mL TNF-α + 50 ng/mL IFN-γ + 25 ng/mL IL-1β + 10 μg/mL LPS) stimulation apically for additional 24 h. Cells were washed and wells were refilled with fresh HBSS buffer. The apical side contains 1 mg/mL of FITC-dextran fluorescein. Absorbance was measured in the basal solution at the indicated time point. The experiments were performed individually at least three times. Data are expressed as mean ± SD. Significant differences between the different concentrations at each time point were analyzed by One-way ANOVA. # $P < 0.00001$

or hatching time variation were observed after exposure to LF up to 250 μg/mL. Although a shorter hatching time was observed at 25 and 100 μg/mL LF, there were no changes of development at any of the tested concentrations. The number of embryos hatched were counted and calculated for the survival rate, presented in Fig. 1C. No statistically significant difference was observed between the indicated concentrations for the survival rate, suggesting the range of LF concentration between 0 μg/mL and 250 μg/mL *in vivo* is not toxic. Based on these data, LF concentrations used in all subsequent experiments were determined to be less than 100 μg/mL, and were concluded to be safe.

Evaluation of paracellular permeability in polarized Caco-2 cells after LF treatment

Maintaining TJ integrity in the intestine is critical for nutrient absorption, host defense, and host immunity. Alteration of intestinal TJ homeostasis is thought to induce pathogenesis of IBD as well as obesity [34]. Since polarized Caco-2 cells have similar structures and functions as intestinal cells and are useful for observation of cell permeability [35], we investigated the effect of LF on the TJ integrity in these cell types. The polarized

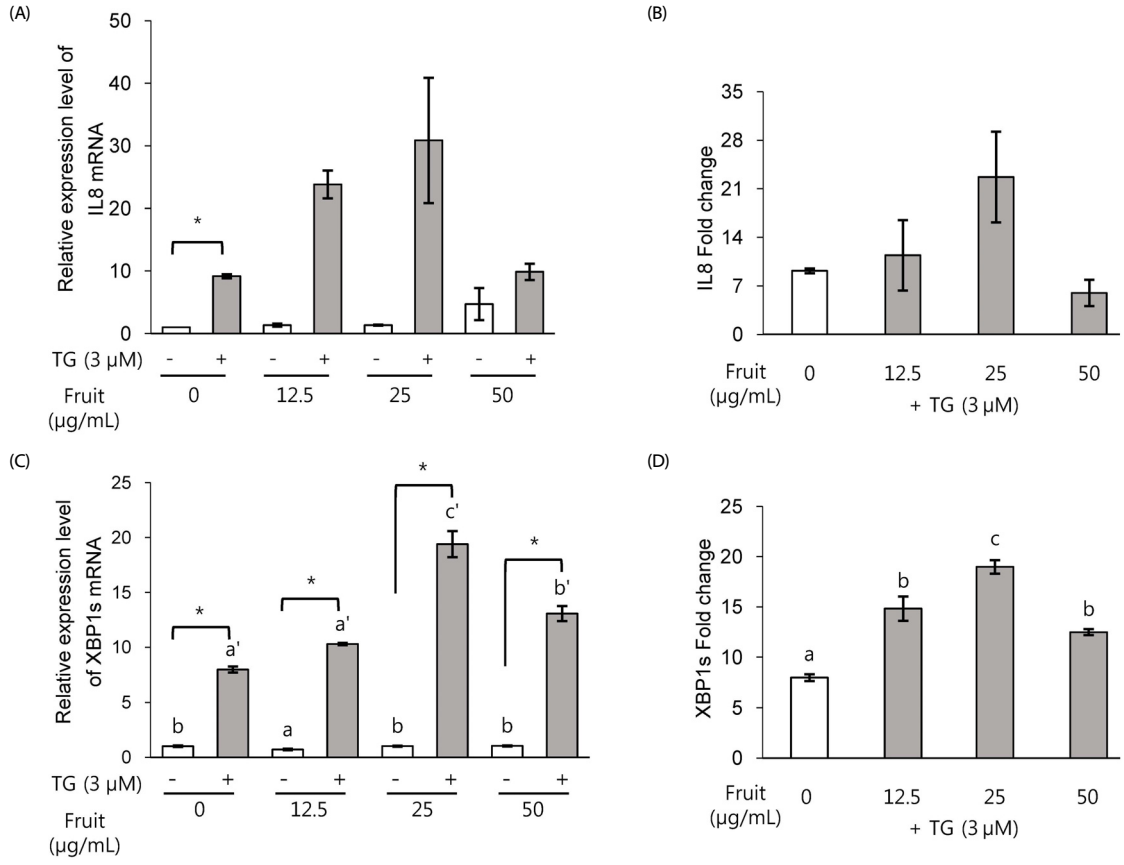

Fig. 3. Effect of LF on expression of IL8 and XBP1s by ER stress in polarized human intestinal epithelial cell. Polarized Caco-2 cells was pretreated with indicated concentrations of LF for 24 h, followed by 3 μM TG stimulation apically for additional 4 h (A and B) or 1 h (C and D). Total RNA was extracted and cDNA prepared for real-time qPCR. Human IL8 (A, B) and XBP1s (C, D) were normalized by human GAPDH. The fold change of IL8 or XBP1s expression induced by TG was calculated at each LF concentration (B, D). The experiments were performed individually at least three times. Data are expressed as mean ± SD. The significant differences between the LF concentrations were analyzed by One-way ANOVA. The TG effect at each concentration was analyzed by student's t-test. * $P < 0.05$. IL8, interleukin 8; XBP1s, X-box binding protein 1 spliced form; GAPDH, glyceraldehyde-3-phosphate dehydrogenase; TG, triglyceride; LF, *L. chinense* fruit.

Caco-2 monolayers were pretreated with LF for 24 h, followed by an additional 24 h incubation without (Fig. 2A) or with (Fig. 2B) cytokine cocktail (50 ng/mL TNF-α + 50 ng/mL IFN-γ + 25 ng/mL IL-1β + 10 μg/mL LPS). Subsequently, 1 mg/mL FITC-dextran was added at the apical section of the chamber, and the fluorescence intensity of the basal chamber was measured to examine the permeability of TJ at each indicated time point. We observed that FITC-dextran in the basal chamber accumulated less significantly in cells pretreated with LF than in untreated cells. Except for 100 μg/mL LF, the accumulated permeation decreased at higher concentrations in a dose-dependent manner (Fig. 2A). Cells stimulated with the cytokines represent the inflammation status in this study. These cells showed a similar pattern, wherein LF pretreatment lowered the permeability of FITC-dextran as compared to the untreated cells, even in the presence of inflammation (Fig. 2B). Taken together, these results indicate that LF has a protective effect of maintaining the TJ integrity of the polarized Caco-2 monolayer, both in the presence and absence of external inflammatory stimuli.

Expression of IL8 by LF in human intestinal epithelial cells

It is well known that ER stress induces a proinflammatory response [36]. To investigate the effect of LF on the expression of proinflammatory cytokines, polarized Caco-2 cells were treated with LF for 24 h, after which ER stress was induced by treatment with 3 μM Thapsigargin (TG). qRT-PCR was performed to examine the expression of representative proinflammatory cytokine IL8, followed by GAPDH normalization (Fig. 3). Compared to untreated cells, cells treated with TG showed significant induction of IL8 (left bars of Fig. 3A), suggesting that TG stimulation works as a positive control in our study. More importantly, we observed that LF itself had no effect on IL8 induction. Fig. 3B shows the fold change by TG stimulation at each concentration of LF pretreatment. A trend was observed for IL8 mRNA expression levels which showed a similar pattern in subsequent experiments, but was statistically not significant ($P > 0.05$).

XBP1 splicing in human intestinal epithelial cells pretreated with LF

To investigate the effect of LF on ER stress, we examined the expression level of XBP1s, an endogenous ER stress-related molecule. As expected, TG significantly induces XBP1s mRNA expression as compared to untreated polarized Caco-2 cells (Fig. 3C). The expression of XBP1s mRNA by LF itself remained

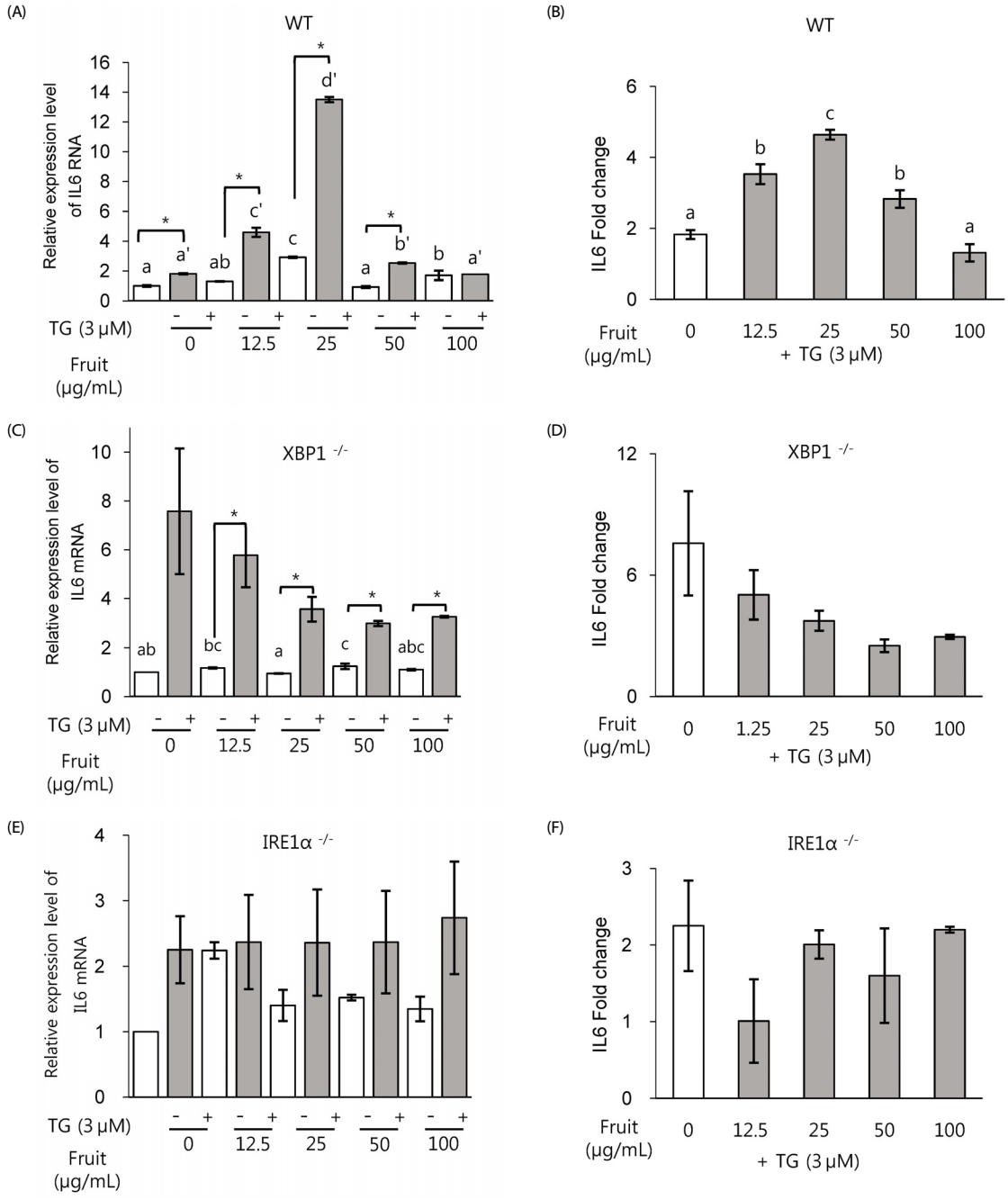

Fig. 4. Effect of LF on proinflammatory response in MEF cells. Wt MEF (A and B), XBP1 KO MEF (C and D) and IRE1α KO MEF (E and F) cell lines were pretreated with LF for 24 h, followed by 3 μM TG for additional 4 h. Total RNA was extracted and cDNA prepared for real-time qPCR. mRNA expression of mouse IL6 (A, C and E) and the fold change of IL6 expression induced by TG (B, D and F) were normalized by mouse β-actin. The experiments were performed individually at least three times. Data are expressed as mean ± SD. Significant differences between the different concentrations were analyzed by One-way ANOVA. The TG effect at each concentration was analyzed by student's t-test. * $P < 0.05$. IL6, interleukin 6; LF, *L. chinense* fruit; TG, triglyceride; XBP1s, X-box binding protein 1 spliced form.

unchanged, except at 12.5 μg/mL concentration. Fig. 3D shows the fold change of XBP1 mRNA induction by TG stimulation is significantly augmented after LF pretreatment. This trend is similar to the IL8 fold change presented in Fig. 3B.

Proinflammatory response by LF in MEF cell lines

MEF knockout (KO) cells lacking each ER stress sensor or marker were used to determine the pathway through which LF regulates the ER stress. mRNA expression levels of IL6 were normalized by β-actin in the same samples.

Expression level of the proinflammatory marker IL6 mRNA, were somewhat changed by LF in wt MEF; however, the variations were not dose-dependent (Fig. 4A). When stimulated with TG, significant induction of IL6 was observed, as compared

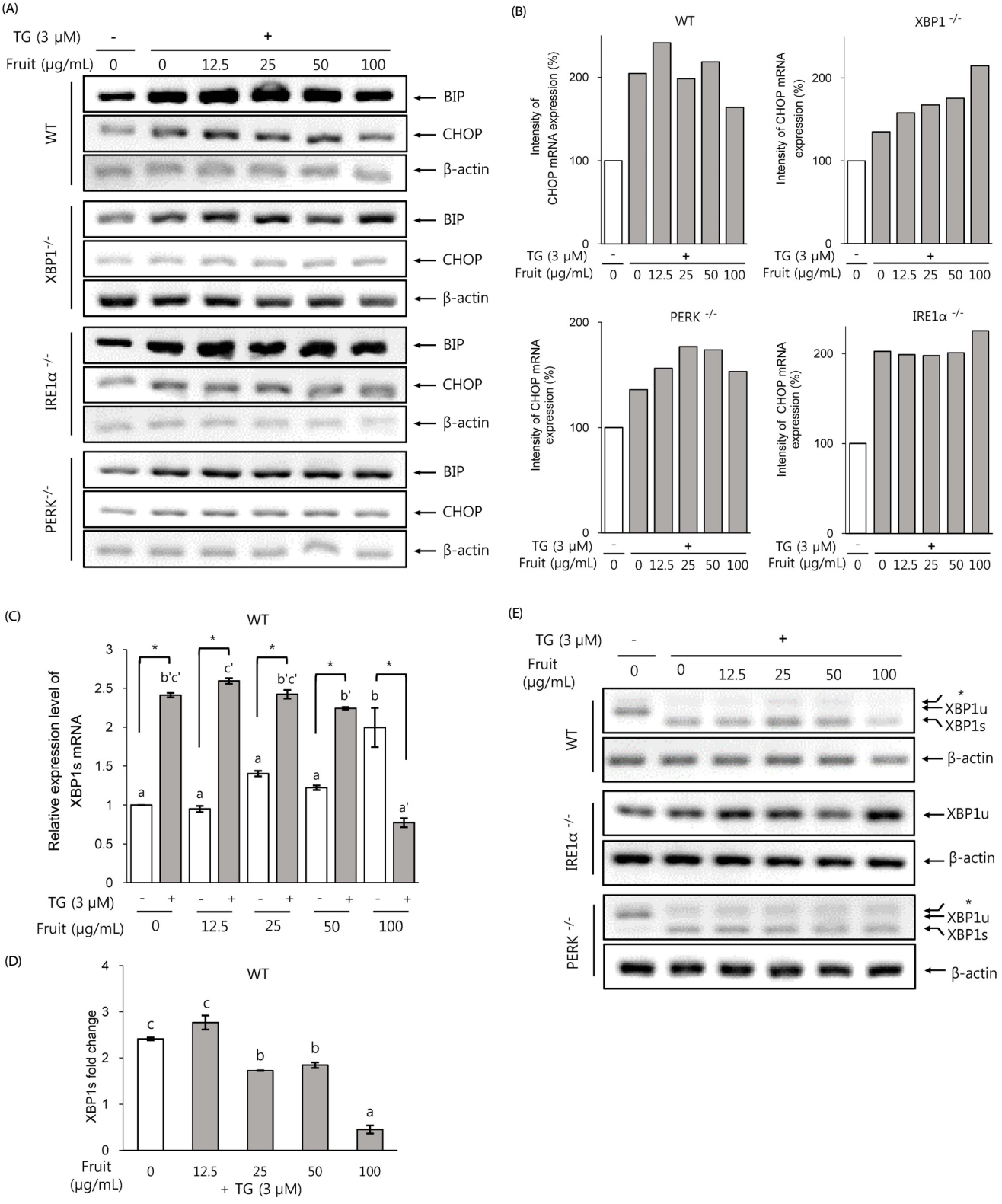

Fig. 5. Effect of LF on the ER stress in MEF cells. MEF cell lines were pretreated with LF for 24 h, followed by 3 μM TG for additional 4 h (A, B) or 1 h (C, D and E). Total RNA was extracted and cDNA prepared for RT-PCR (A and E) and real-time qPCR (C, D). Mouse CHOP, XBP1s mRNA expression were normalized by mouse β-actin (B, C and D); CHOP mRNA expression was quantified using the ImageJ software (B). The experiments were performed individually at least three times. Data are expressed as mean ± SD. Significant differences between the different concentrations were analyzed by One-way ANOVA. The TG effect at each concentration was analyzed by student's t-test. * $P < 0.05$. BiP, Immunoglobulin binding protein; CHOP, CCAAT/enhancer-binding homologous protein; XBP1s, X-box binding protein 1 spliced form.

to the control group (Fig. 4A). The fold change of IL6 by TG stimulation were significantly augmented in the range 12.5-50 μg/mL concentration of LF (Fig. 4B). However, in MEF cells lacking XBP1, although LF itself exerted some effect on the IL6 mRNA expression, it was not dose-dependent. Conversely, treatment with TG significantly induced IL6 mRNA expression levels at all LF concentrations (Fig. 4C). However, no significant change of IL6 induction by LF with TG stimulation was observed in the absence of XBP1, suggesting regulation through an XBP1-dependent inflammatory pathway by LF (Fig. 4D). Fig. 4E and 4F reveal that IRE1α KO MEF cells show no significant changes or notable patterns in IL6 mRNA level after exposure to either LF or TG, suggesting an IRE1α-dependent inflammatory pathway. In summary, these results show that LF increases the proinflammatory response through an IRE1α-XBP1-dependent manner in the presence of ER stress between the ranges 12.5-50 μg/mL LF.

Expression of ER stress markers in MEF KO cells

Our previous experiment reveals that LF regulates the inflammatory response via the IRE1α-XBP1-pathway on ER stress mechanism. Therefore, we next investigated the effect of LF on ER stress hallmarks BiP and CHOP in MEF KO cells.

In Fig. 5A, we present the ER stress hallmarks affected by LF. As expected, TG induces the expression of BiP, a representative ER stress marker, in all MEF cell lines (Fig. 5A). TG also induces CHOP, a representative apoptosis and ER stress marker, in all the MEF cell lines except XBP1 KO MEF. The relative intensity of the CHOP bands was calculated using the Image J software (Fig. 5B). We observed that high concentration of LF (100 μg/mL) inhibited the CHOP mRNA expression induced by TG in wt MEF and PERK KO MEF, as compared to XBP1 KO MEF and IRE1α KO MEF. This pattern is similar to expression levels of IL6 in wt MEF, and IL8 and XBP1s in polarized Caco-2 cells. This result therefore suggests that LF activates the survival mode of ER stress mechanism in an IRE1α-XBP1-dependent manner, but with no involvement of the PERK pathway (Fig. 5B).

Since LF regulates the proinflammatory response via XBP1 pathway, we further examined the expression of XBP1s by applying qRT-PCR. Fig. 5C shows that TG significantly induces the expression of XBP1s mRNA in wt MEF. In the absence of TG, the expression level of XBP1 mRNA by LF itself was not significantly changed, except at 100 μg/mL concentration of LF. However, the fold change of XBP1s mRNA induced by TG significantly decreases in a dose-dependent manner, which suggests that LF dose-dependently inhibits XBP1s in the presence of ER stress (Fig. 5D). The RT-PCR data of Fig. 5E confirms the qRT-PCR results presented in Fig 5D. The unspliced form of XBP1 (XBP1u) is seen as the upper band and the spliced form of XBP1 (XBP1s) is the lower band. Note that TG treatment shows the lower molecular weight of band (XBP1s) while the negative control shows only the higher molecular weight of band (XBP1u) in wt MEF. Since RT-PCR is not as sensitive as qRT-PCR, exposure to 100 μg/mL LF reveals only a weak band. Pretreatment of IRE1α KO MEF cells with LF showed no induction of XBP1s by TG, since IRE1α is upstream of the XBP1 molecule, and XBP1u cannot be cleaved to the spliced form in the absence of IRE1α. PERK KO MEF cells treated with LF were observed to induce XBP1s by TG, but the effect was not dose-dependent with respect to LF concentration (Fig. 5E, lower panel). Therefore, in the absence of PERK and IRE1α, no changes were observed in the levels of XBP1s after LF exposure. This suggests that LF inhibits XBP1 splicing in the presence of ER stress. Also, these results confirm the data presented in Fig. 5A, that LF does not exert its effect in regulating the inflammatory response or ER stress via the PERK pathway.

Taken together, our results indicate that 12.5-50 μg/mL of LF induces IRE1α-XBP1-dependent inflammation and inhibits XBP1s for the survival pathway; however, above 50 μg/mL, LF alters to the opposition effect by inhibiting the proinflammatory response and inducing CHOP expression, resulting in apoptosis. These are very interesting results that reveal the dose-dependent dual effect of LF.

Changes on the cell surface after treatment with LF or TG

Since the first reports of SICM imaging [37], multiple studies have reported SICM imaging of various biological samples, including cultured cells [38-41]. These previous findings indicate that SICM is a useful tool for imaging the surface topography of living and fixed cultured cells at nanoscale resolution under liquid. We utilized this new imaging technique to examine the condition of cells in experiments and the effects of any reagent (namely, LF in this study) on the surface morphology of the single cell. We obtained excellent image quality of SICM for fixed single MEF cells, thereby corroborating its potential for future studies. SICM image of intact MEF cells under various conditions indicate that the KO of XBP1 or IRE1α, and treatment of LF or TG, does not have any acute detrimental effects on the cells (Supplementary Fig. 1A). However, surprisingly, the surface of IRE1α KO MEF shows increased cytoskeleton polymer-like structures as compared to other KO MEF cell lines, indicating that knock-out IRE1α (which is ER the transmembrane sensor protein) possibly has some effect on the morphological changes, and this requires further investigation (Supplementary Fig. 1B).

DISCUSSION

LF found in China mainly has a sweet taste. Dried LF has long been used by the ancient Chinese to help the function of eyes, liver, kidneys and lungs. Furthermore, scientific studies for the *Lycium barbarum* fruit has proven its beneficial effects on immunomodulation, hypoglycemia, hypolipidemia, antiaging and antitumor properties [42-44].

In this study, we focused on LF exerting its protective function on the gut barrier as well as against inflammation and ER stress in the intestine of humans. Our results indicate that LF protects the intestinal barrier significantly, both in the presence and absence of an inflammatory environment (Fig. 2). Although it was not statistically significant in Caco-2 cells, both MEF cell lines and Caco-2 cells showed a similar pattern of proinflammatory response along with ER stress response. The low dose of LF increased the proinflammatory response in the presence of ER stress, while at high concentrations exceeding 50 μg/mL showed no change. We believe this finding reveals a biological phenotype of the LF effect. Moreover, this effect is XBP1 dependent, implying that LF regulates inflammatory response

by XBP1 through the IRE1α-XBP1 pathway followed by inhibiting ER stress and further inflammation.

As seen in Fig. 5C, the highest concentration of LF (100 μg/mL) itself induces XBP1s significantly, even in the absence of TG. We therefore conclude that higher concentrations of LF by itself are capable of inducing ER stress or general toxicity. This might be due to the survival/protection mode of the cell by activating ER stress and other protection mechanisms. However, this phenomenon needs to be followed up by further investigations.

Taken together, our results show the beneficial effect of LF on human intestine by exerting a protective function on the gut barrier, and regulation of inflammation induced by ER stress in an IRE1α-XBP1-dependent manner. In addition, AFM data shows no morphological changes by LF on MEF cells, suggesting that LF does not change or interfere with the activity with respect to cell surface morphology. However, it is interesting to note that in the absence of the ER transmembrane protein IRE1α, the cell surface is altered. Further detailed mechanistic studies are required to confirm our data regarding the influence of IRE1α on the cell surface plasma membrane, including microtubules.

CONFLICT OF INTEREST

The authors declare no potential conflicts of interest

ORCID

So-Rok Lee: https://orcid.org/0000-0001-9917-6652
Hye-Jeong Hwang: https://orcid.org/0000-0002-1948-4442
Ju-Gyeong Yoon: https://orcid.org/0000-0001-6030-4565
Eun-Young Bae: https://orcid.org/0000-0003-1844-1296
Kyo-Suk Goo: https://orcid.org/0000-0002-3815-0763
Sang-Joon Cho: https://orcid.org/0000-0003-4822-5658
Jin Ah Cho: https://orcid.org/0000-0001-9265-2409

REFERENCES

1. Ellgaard L, Molinari M, Helenius A. Setting the standards: quality control in the secretory pathway. Science 1999;286:1882-8.
2. Stengel S, Messner B, Falk-Paulsen M, Sommer N, Rosenstiel P. Regulated proteolysis as an element of ER stress and autophagy: implications for intestinal inflammation. Biochim Biophys Acta Mol Cell Res 2017;1864:2183-90.
3. Hampton RY. ER stress response: getting the UPR hand on misfolded proteins. Curr Biol 2000;10:R518-21.
4. Welihinda AA, Kaufman RJ. The unfolded protein response pathway in Saccharomyces cerevisiae. Oligomerization and trans-phosphorylation of Ire1p (Ern1p) are required for kinase activation. J Biol Chem 1996;271:18181-7.
5. Oakes SA, Papa FR. The role of endoplasmic reticulum stress in human pathology. Annu Rev Pathol 2015;10:173-94.
6. Vembar SS, Brodsky JL. One step at a time: endoplasmic reticulum-associated degradation. Nat Rev Mol Cell Biol 2008;9:944-57.
7. Urano F, Wang X, Bertolotti A, Zhang Y, Chung P, Harding HP, Ron D. Coupling of stress in the ER to activation of JNK protein kinases by transmembrane protein kinase IRE1. Science 2000;287:664-6.
8. Zinszner H, Kuroda M, Wang X, Batchvarova N, Lightfoot RT, Remotti H, Stevens JL, Ron D. CHOP is implicated in programmed cell death in response to impaired function of the endoplasmic reticulum. Genes Dev 1998;12:982-95.
9. Luo K, Cao SS. Endoplasmic reticulum stress in intestinal epithelial cell function and inflammatory bowel disease. Gastroenterol Res Pract 2015;2015:328791.
10. Hosomi S, Kaser A, Blumberg RS. Role of endoplasmic reticulum stress and autophagy as interlinking pathways in the pathogenesis of inflammatory bowel disease. Curr Opin Gastroenterol 2015;31:81-8.
11. Ng SC, Tang W, Ching JY, Wong M, Chow CM, Hui AJ, Wong TC, Leung VK, Tsang SW, Yu HH, Li MF, Ng KK, Kamm MA, Studd C, Bell S, Leong R, de Silva HJ, Kasturiratne A, Mufeena MNF, Ling KL, Ooi CJ, Tan PS, Ong D, Goh KL, Hilmi I, Pisespongsa P, Manatsathit S, Rerknimitr R, Aniwan S, Wang YF, Ouyang Q, Zeng Z, Zhu Z, Chen MH, Hu PJ, Wu K, Wang X, Simadibrata M, Abdullah M, Wu JC, Sung JJY, Chan FKL; Asia-Pacific Crohn's and Colitis Epidemiologic Study (ACCESS) Study Group. Incidence and phenotype of inflammatory bowel disease based on results from the Asia-pacific Crohn's and colitis epidemiology study. Gastroenterology 2013;145:158-65.e2.
12. Mulder DJ, Noble AJ, Justinich CJ, Duffin JM. A tale of two diseases: the history of inflammatory bowel disease. J Crohns Colitis 2014;8:341-8.
13. Cao SS, Zimmermann EM, Chuang BM, Song B, Nwokoye A, Wilkinson JE, Eaton KA, Kaufman RJ. The unfolded protein response and chemical chaperones reduce protein misfolding and colitis in mice. Gastroenterology 2013;144:989-1000.e6.
14. Dixon LJ, Kabi A, Nickerson KP, McDonald C. Combinatorial effects of diet and genetics on inflammatory bowel disease pathogenesis. Inflamm Bowel Dis 2015;21:912-22.
15. Neish AS. Microbes in gastrointestinal health and disease. Gastroenterology 2009;136:65-80.
16. Kaser A, Lee AH, Franke A, Glickman JN, Zeissig S, Tilg H, Nieuwenhuis EE, Higgins DE, Schreiber S, Glimcher LH, Blumberg RS. XBP1 links ER stress to intestinal inflammation and confers genetic risk for human inflammatory bowel disease. Cell 2008;134:743-56.
17. Chassaing B, Darfeuille-Michaud A. The commensal microbiota and enteropathogens in the pathogenesis of inflammatory bowel diseases. Gastroenterology 2011;140:1720-8.
18. Cho JH, Brant SR. Recent insights into the genetics of inflammatory bowel disease. Gastroenterology 2011;140:1704-12.
19. Jostins L, Ripke S, Weersma RK, Duerr RH, McGovern DP, Hui KY, Lee JC, Schumm LP, Sharma Y, Anderson CA, Essers J, Mitrovic M, Ning K, Cleynen I, Theatre E, Spain SL, Raychaudhuri S, Goyette P, Wei Z, Abraham C, Achkar JP, Ahmad T, Amininejad L, Ananthakrishnan AN, Andersen V, Andrews JM, Baidoo L, Balschun T, Bampton PA, Bitton A, Boucher G, Brand S, Büning C, Cohain A, Cichon S, D'Amato M, De Jong D, Devaney KL, Dubinsky M, Edwards C, Ellinghaus D, Ferguson LR, Franchimont D, Fransen K, Gearry R, Georges M, Gieger C, Glas J, Haritunians T, Hart A, Hawkey C, Hedl M, Hu X, Karlsen TH, Kupcinskas L, Kugathasan S, Latiano A, Laukens D, Lawrance IC, Lees CW, Louis E, Mahy G, Mansfield J, Morgan AR, Mowat C, Newman W, Palmieri O, Ponsioen CY, Potocnik U, Prescott NJ, Regueiro M, Rotter JI, Russell RK, Sanderson JD, Sans M, Satsangi J, Schreiber S, Simms LA, Sventoraityte J, Targan SR, Taylor KD, Tremelling M, Verspaget HW, De Vos M,

Wijmenga C, Wilson DC, Winkelmann J, Xavier RJ, Zeissig S, Zhang B, Zhang CK, Zhao H; International IBD Genetics Consortium (IIBDGC), Silverberg MS, Annese V, Hakonarson H, Brant SR, Radford-Smith G, Mathew CG, Rioux JD, Schadt EE, Daly MJ, Franke A, Parkes M, Vermeire S, Barrett JC, Cho JH. Host-microbe interactions have shaped the genetic architecture of inflammatory bowel disease. Nature 2012;491:119-24.

20. Lee SH. Intestinal permeability regulation by tight junction: implication on inflammatory bowel diseases. Intest Res 2015;13:11-8.
21. Wu GD, Bushmanc FD, Lewis JD. Diet, the human gut microbiota, and IBD. Anaerobe 2013;24:117-20.
22. O'Sullivan M, O'Morain C. Nutrition in inflammatory bowel disease. Best Pract Res Clin Gastroenterol 2006;20:561-73.
23. Halmos EP, Christophersen CT, Bird AR, Shepherd SJ, Gibson PR, Muir JG. Diets that differ in their FODMAP content alter the colonic luminal microenvironment. Gut 2015;64:93-100.
24. Gilardi D, Fiorino G, Genua M, Allocca M, Danese S. Complementary and alternative medicine in inflammatory bowel diseases: what is the future in the field of herbal medicine? Expert Rev Gastroenterol Hepatol 2014;8:835-46.
25. Langhorst J, Wulfert H, Lauche R, Klose P, Cramer H, Dobos GJ, Korzenik J. Systematic review of complementary and alternative medicine treatments in inflammatory bowel diseases. J Crohns Colitis 2015;9:86-106.
26. Hu S, Ciancio MJ, Lahav M, Fujiya M, Lichtenstein L, Anant S, Musch MW, Chang EB. Translational inhibition of colonic epithelial heat shock proteins by IFN-γ and TNF-α in intestinal inflammation. Gastroenterology 2007;133:1893-904.
27. Yao R, Heinrich M, Zou Y, Reich E, Zhang X, Chen Y, Weckerle CS. Quality variation of Goji (fruits of Lycium spp.) in China: a comparative morphological and metabolomic analysis. Front Pharmacol 2018;9:151.
28. Yao R, Heinrich M, Weckerle CS. The genus Lycium as food and medicine: a botanical, ethnobotanical and historical review. J Ethnopharmacol 2018;212:50-66.
29. Amagase H, Farnsworth NR. A review of botanical characteristics, phytochemistry, clinical relevance in efficacy and safety of Lycium barbarum fruit (Goji). Food Res Int 2011;44:1702-17.
30. Chang RC, So KF. Use of anti-aging herbal medicine, Lycium barbarum, against aging-associated diseases. What do we know so far? Cell Mol Neurobiol 2008;28:643-52.
31. Wang CC, Chang SC, Inbaraj B, Stephen Chen BH. Isolation of carotenoids, flavonoids and polysaccharides from Lycium barbarum L. and evaluation of antioxidant activity. Food Chem 2010;120: 184-92.
32. Chan HC, Chang RC, Koon-Ching Ip A, Chiu K, Yuen WH, Zee SY, So KF. Neuroprotective effects of Lycium barbarum Lynn on protecting retinal ganglion cells in an ocular hypertension model of glaucoma. Exp Neurol 2007;203:269-73.
33. Luo Q, Cai Y, Yan J, Sun M, Corke H. Hypoglycemic and hypolipidemic effects and antioxidant activity of fruit extracts from Lycium barbarum. Life Sci 2004;76:137-49.
34. Nagpal R, Newman TM, Wang S, Jain S, Lovato JF, Yadav H. Obesity-linked gut microbiome dysbiosis associated with derangements in gut permeability and intestinal cellular homeostasis independent of diet. J Diabetes Res 2018;2018:3462092.
35. Ferraretto A, Bottani M, De Luca P, Cornaghi L, Arnaboldi F, Maggioni M, Fiorilli A, Donetti E. Morphofunctional properties of a differentiated Caco2/HT-29 co-culture as an in vitro model of human intestinal epithelium. Biosci Rep 2018;38:BSR20171497.
36. Garg AD, Kaczmarek A, Krysko O, Vandenabeele P, Krysko DV, Agostinis P. ER stress-induced inflammation: does it aid or impede disease progression? Trends Mol Med 2012;18:589-98.
37. Korchev YE, Bashford CL, Milovanovic M, Vodyanoy I, Lab MJ. Scanning ion conductance microscopy of living cells. Biophys J 1997;73:653-8.
38. Rheinlaender J, Geisse NA, Proksch R, Schäffer TE. Comparison of scanning ion conductance microscopy with atomic force microscopy for cell imaging. Langmuir 2011;27:697-704.
39. Gorelik J, Zhang Y, Shevchuk AI, Frolenkov GI, Sánchez D, Lab MJ, Vodyanoy I, Edwards CR, Klenerman D, Korchev YE. The use of scanning ion conductance microscopy to image A6 cells. Mol Cell Endocrinol 2004;217:101-8.
40. Ushiki T, Nakajima M, Choi M, Cho SJ, Iwata F. Scanning ion conductance microscopy for imaging biological samples in liquid: a comparative study with atomic force microscopy and scanning electron microscopy. Micron 2012;43:1390-8.
41. Anariba F, Anh JH, Jung GE, Cho NJ, Cho SJ. Biophysical applications of scanning ion conductance microscopy (SICM). Mod Phys Lett B 2012;26:1130003.
42. Gan L, Hua Zhang S, Liang Yang X, Bi Xu H. Immunomodulation and antitumor activity by a polysaccharide-protein complex from Lycium barbarum. Int Immunopharmacol 2004;4:563-9.
43. Jing L, Cui G, Feng Q, Xiao Y. Evaluation of hypoglycemic activity of the polysaccharides extracted from Lycium barbarum. Afr J Tradit Complement Altern Med 2009;6:579-84.
44. Zhang Z, Liu X, Zhang X, Liu J, Hao Y, Yang X, Wang Y. Comparative evaluation of the antioxidant effects of the natural vitamin C analog 2-O-β-D-glucopyranosyl-L-ascorbic acid isolated from Goji berry fruit. Arch Pharm Res 2011;34:801-10.